

Design of Vibratory MEMS Gyroscope with Crab Leg Flexure Anchors for High Sensitivity

Sudha R Karbari

Assistant Professor, RV College of Engineering, Bangalore
(karbari.rsudha@gmail.com)

Abstract- A Highly sensitive MEMS Gyroscope is proposed in this paper with the translational axis being along Z-axis. A comparative study of the designs in terms of sensitivity and displacement. Eigen frequency analysis is being carried out for frequency tuning of sense mode and drive mode to increase the sensitivity. Here we are trying to match the two mode frequencies for the same. With reference to change in its mechanical structure, there is a change in displacement when a dc voltage is applied and the quadrature error in the micro machined vibrating is also minimized. The design is modified and the mechanical structure dimensions are chosen such that sensitivity varies with the addition of serpentine beams. The simulation results predict the resonant frequency to be very low indicating high sensitivity for frequencies of the order of 10 KHz to 2.82 KHz. With still more variations in the design parameters such as the length of serpentine, the resonant frequencies of drive and sense mode changes with respect to change in input angular moment in the Z-direction. In our designs of structures the resonant frequencies varies from 10KHz to 2.8 KHz. Resonant frequencies of a design play a major role in increasing the sensitivity of the device. The Bandwidth is around 200 Hz with displacement of 0.01 microns. The applied dc voltage is 10V and the ac voltage being 2 V along the plates. In this paper we are also discussing about the displacements for various structures along with the frequency analysis.

Keywords- MEMS, Sensitivity, Crab Leg Flexures

I. INTRODUCTION

MICRO ELECTROMECHANICAL SYSTEMS gyros has been attracting lot of attention for its applications in various fields that demand low cost, and compact size. Some of the applications as of such are automotive safety systems, Inertial Navigation Systems, Consumer electronics, Automotive applications, GPS augmentation and a wide range of new military applications.[1] Today's gyros are vibratory in nature that have structures fabricated on crystal silicon or a poly silicon making them more compact and cost efficient with low power consumption for many applications.[2] But the parameters such as undesired mechanical coupling between the two modes during matched mode is drastically reduced by fully decoupling the gyroscope flexures along both the X and Y

directions. Hence the reduced coupling results in a stable zero output bias improving bias stability.[3]

In a resonant MEMS gyro the sensitivity is maximized when drive and sense frequencies match, however practically due to fabrication imperfections and mechanical tolerances this is not achieved. Even though the gyro uses same spring along sense and drive directions there is always a remarkable difference between them that is unavoidable [4].

Further to add on a MEMS gyro retains the wide range of bandwidth for a symmetric shape of proof mass and comb fingers. The branch fingers along the drive and sense direction act as stiffness tuners. Here we are using the drive and sense direction voltage to control the tuning between two direction for a wide range of frequencies.[5] In future, the next generation high performance MEMS devices will require fabrication technologies that combine high aspect ratio deep dry etching techniques with poly silicon surface micromachining to realize all silicon thick microstructures electrically isolated from each other and separated by small capacitive gaps. Fabrication of large area, vertical capacitors with micron gaps increase the sensitivity by the orders of magnitude.[6] Three parameters that define the primary performance of MEMS gyro are Sensitivity, Resolution and Stability. An analysis of these parametric analysis begins with a phenomenon called Coriolis force. When a structure moves in a rotating frame along X direction naming it as drive direction and an angular rotation is applied along the Y direction then the structure experiences Coriolis force along a direction perpendicular to both X and Y direction i.e. along the Z direction naming it as sense direction. Now let us define the Coriolis force as the product of mass of the structure of proof mass and the acceleration.

$$F=ma \quad (1)$$

Where m is mass of the proof mass of structure. The Coriolis acceleration 'a' being proportional to the velocity 'v' of moving structure and rotating rate ' Ω ' of the rotating frame.

$$a=2v \times \Omega \quad (2)$$

A model of vibrating MEMS gyroscope is shown in figure 1. The suspensions along both the axis provide appropriate elastic stiffness and constraints in a such a way that the proof mass relative to the frame moves in Z axis sense direction and

frame relative to the die moves in X axis drive direction also called as rotating frame.

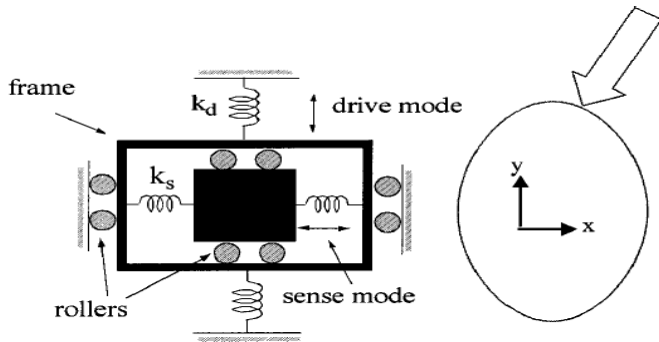


Figure 1. The two dimensional spring-mass-damper system showing the sense and drive directions.[7]

The main advantage of decreasing the resonant frequency f_0 of MEMS gyro is to significantly increase the sensitivity and reduction of quadrature error as a major advantage. Design alternatives to increase sensitivity are reducing the modal frequencies by varying the dimensions of the sensing element.[7].

Different Factors affecting the sensitivity of MEMS gyroscope are Q factor, Decoupling modes, resonant frequencies and fabrication imperfections. In our design, for the proof mass we are much more analyzing towards mode matching of resonant frequencies of sense and drive directions. Eigen frequency analysis is modal frequency analysis at which the structure vibrates the maximum. So we are going for modal analysis to know the vibrations of the proof mass and give different deflections in terms of displacements.[8].

II. DESIGN1

A. Design specifications.

The TABLE 1 shows the various dimensions of the proof mass, comb drive along the sense, comb drives along drive direction, dimensions of Suspension crab flexures and perforations.

B. Process File

The static variables considered here are pressure and temperature of 101.325 k Pa and 273.15 degrees. The below figure 2. shows the process field of MEMS gyroscope with both Si as a substrate and as a proof mass. Upon the 50 micron Si substrate there is a proof mass of having a thickness of 30 micron in between having a gap of 1 micron oxide layer.

TABLE I. DIMENSIONS OF PROOF MASS.

Name of the components	Dimensions in microns
Proof mass	Length=600 Width=600
Comb Drive along drive direction	Length=400 Width=50 Pitch=135 Overlap=100
Comb Drive along Sense direction	Length=110 Width=5 Pitch=20 Edge width=400 Overlap=100
L Suspension	Length=250 Width=5
Holes	Length=20 Width=20 Spacing=10

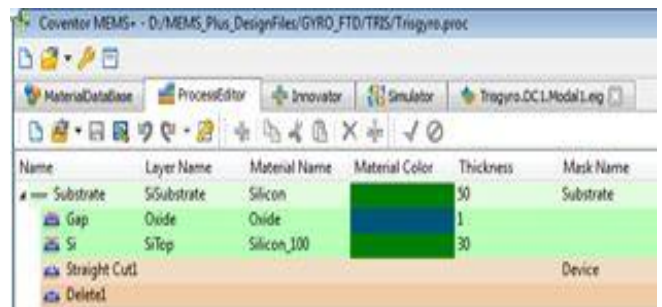


Figure 2. Process file of MEMS gyroscope in MEMS+ window

C. Modelling and frequency analysis of Design 1

After defining the process, we are modeling the design in the innovator tab of MEMS+ as shown in figure 3. This is done by first exposing the variables in the variables tab. Now after declaring the variables, components are formed by using different rigid plate, beams and rectangular segments etc.

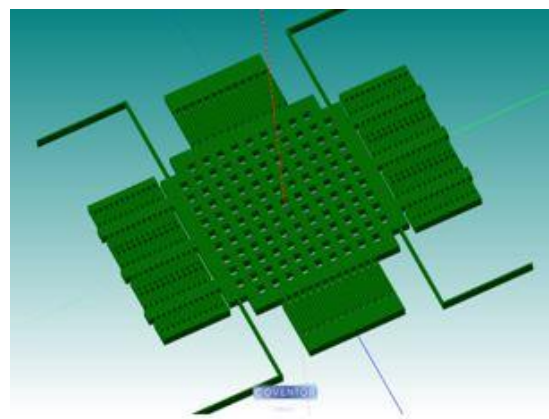


Figure 3. 3-Dimensional Simulation of Design1.

The design 1 shows the L suspensions included along all the four corners of the proof mass of length 250 microns and width of 5 microns. The comb drives along the sense and drive direction are not the same which makes a conclusion that our design is only symmetric along the proof mass but not along the comb drives. For symmetric structures the resonant modes of drive and sense match contribute to mode matching. The proof mass dimensions are also tweaked in to meet the specifications required. Here we have targeted a resonant frequency of 10 K Hz. We were able to meet the specifications with this design, but the displacement is not so appreciable. The modal frequencies are as follows in TABLE 2.

TABLE II. SHOWING THE MODES WITH THEIR RESPECTIVE FREQUENCIES.

Modes	Frequencies in K Hz
Sense	10.157
Drive	10.209
Z axis	27.980

The figure 4 shows the displacement and frequency of the drive mode of 10.209 KHz along Y direction.

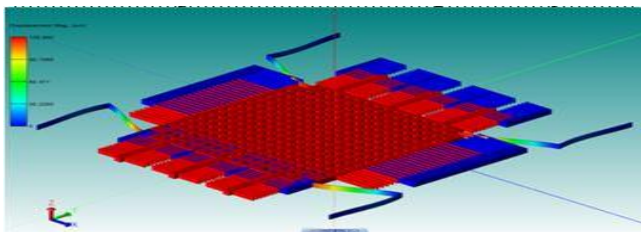


Figure 4. modal frequency along the drive direction of design1.

The figure 5 gives us an overview of the displacements and frequencies along the Z axis with the resonant frequency being 27.980 KHz.

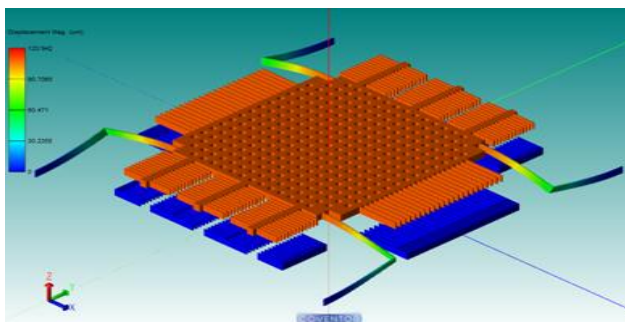


Figure 5. modal frequency along the sense direction of design 1.

From below figure 6 displayed in the COVENTOR window, we can conclude on the values of displacement and resonant frequency along the X direction which is 10.157 KHz.

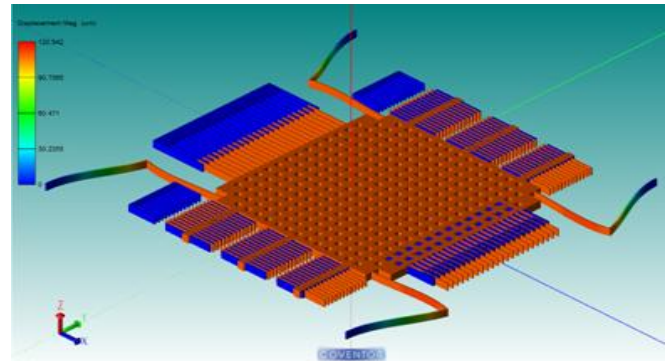


Figure 6. modal frequency along Z direction of design 1.

Now we have also verified the result of resonant frequencies by simulating the same design in COVENTOR which gives us the FEM(*finite element analysis*) analysis. Comparing the results of MEMS+ with that of the FEM results as shown below. As our main concern is to match the resonant frequencies we have only done modal analysis here.

C modeDomain			
	Frequency	Generalized Mass	Damping
1	1.16672E04	1.916535E-08	0
2	1.180192E04	1.920851E-08	0
3	1.422232E04	6.491691E-09	0

Figure 7. Modal Frequencies of design1 FEM analysis.

From TABLE 3 we conclude that the sense and drive modal frequencies are in match with each other. Now our next concern is to increase the displacement for the DC voltage applied. To do that apply AC along X axis drive direction along with dc applied to electrical connectors.

TABLE III. COMPARISON RESULTS OF MODAL FREQUENCIES IN MEMS+ AND FEM.

Frequency in KHz	MEMS+	FEM
Sense	10.157	11.66
Drive	10.209	11.80
Z-axis	27.980	14.22

D. AC/DC analysis of Design 1.

In the next step we have applied a dc voltage of 5 V and noted down the displacement for the same which is 0.0003 microns. As can be seen from the simulated results, it is evident that there is not much displacement. So went on to include serpentines instead of straight beams. As can be seen from the figure the displacement has increased along the drive direction to .00612 micron. But along the sense direction and Z axis it is still low as in the following figures.

The figure 8 shows the plot of displacement versus frequency with a maximum displacement occurring at 10 KHz peak value. The value of displacement is 0.00612 micron which is very less and hence there is a need for optimization of the design in terms of structural mechanics.

The figure 9 shows the displacement along the y axis being 7.4 e-23 micron occurring at 10 KHz. So in order to overcome this and increase the displacement we have optimized our design to make it more flexible and hence forth reduce the spring constant of the design and improve the displacement.

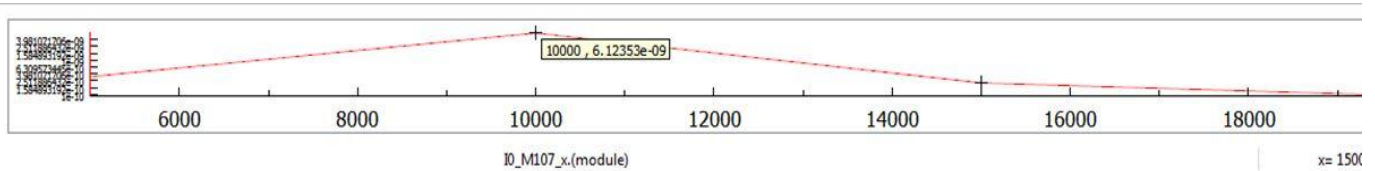


Figure 8. Maximum displacement along x axis is 6.12e-9 for design 1.

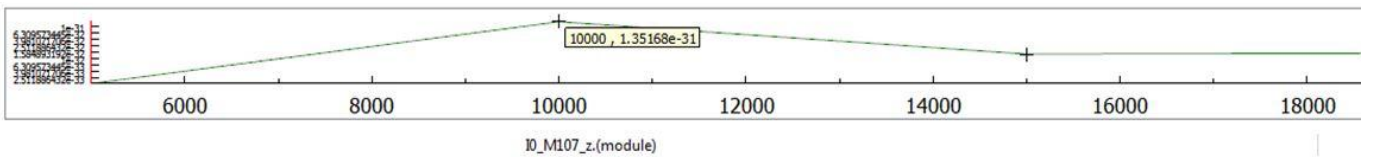


Figure 9. Maximum displacement result along y axis of design 1.

Similarly the displacement along the resonant frequency of the order of e^{-31} along the Z axis and next we proceed towards finding the AC and DC voltages required to actuate the device for the accurate displacement and working frequency. For the complete AC voltage analysis we are varying dc bias from 0 to 20 V for AC of 2 V and 180 phase shift between x and y axis that is depicted in figure 10.

displacement values are very low and hence need to be enhanced. Along with this we also want to reduce the resonant frequencies to increase the sensitivity of design.

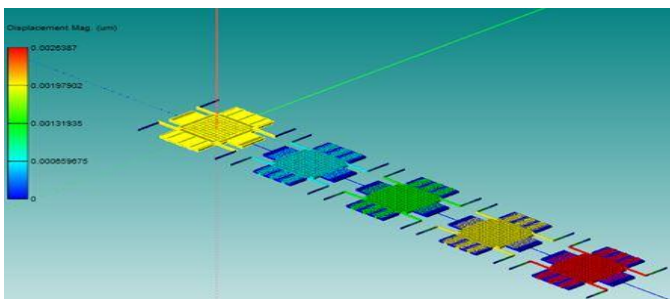


Figure 10. Maximum displacement along the Z axis with change in Voltage bias.

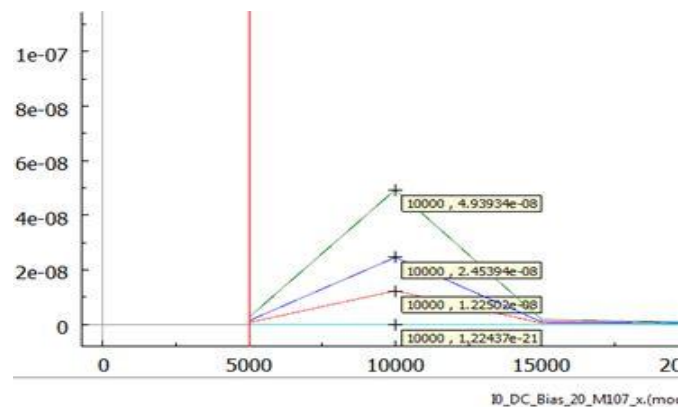


Figure 11. Plot of displacement v/s frequency for different DC and AC voltages

In figure 11 we have voltage analysis for design 1 from 0 V to 20 V in steps of 4, so we have 5 different models of design 1 with respect to change in voltage values to simulate. From the above analysis we conclude that the

Next step we have increased the number of iterations from 5 to 8 and observed for what different values of DC voltages we get the appreciable displacement as can be seen from figure 12.

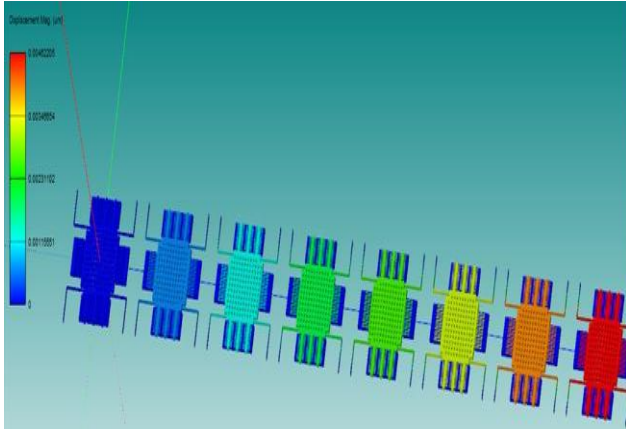


Figure 12. Maximum displacement along Z axis for different voltage bias.

Figure 13 shows the plot of displacement versus frequencies that the values of displacements have increased for increase in the supply voltages used to actuate the device. now changed the range of DC voltage applied from 0 to 35 with steps of 5 giving us 8 iterations.

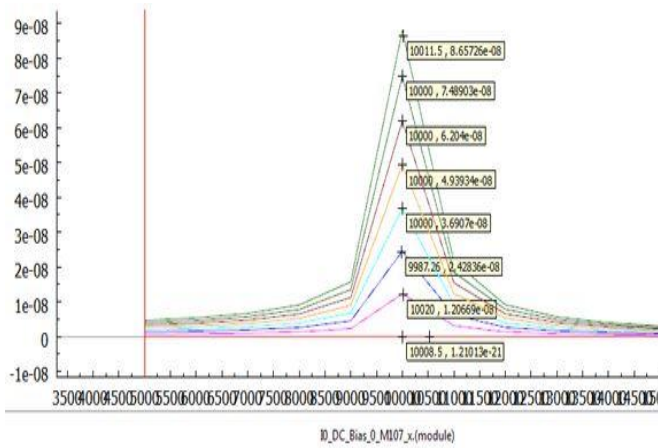


Figure 13. Plot of displacement versus frequency for different 8 DC voltages

Figure 14 shows the displacement is at 6.526×10^{-6} microns for ac input of 6 V and dc of 5 V. This occurs at 10.209 KHz.

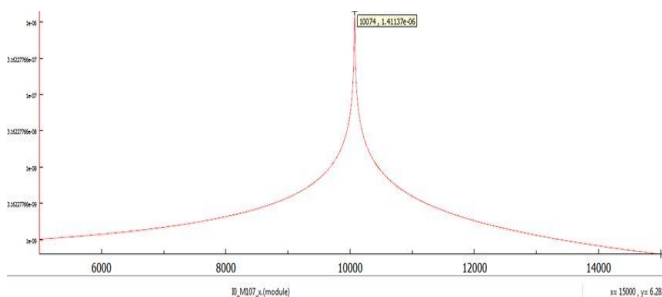


Figure 14. Maximum displacement in micron for AC and DC varied.

III. DESIGN 2

The proof mass size is also increased by increasing the length and breadth of it by 100 microns each. As the area is increased, mass is increased as shown in figure 15. As the resonant frequencies and the generalized mass are inversely proportional to each other, increasing in one entity decreases the other. Hence the resonant frequency is reduced. This is very evident from the tabulated results below. Along with the change in the dimensions of proof mass, we also included serpentine to make the design more flexible. This is done to increase the displacement for the DC voltage applied which is 5 V.

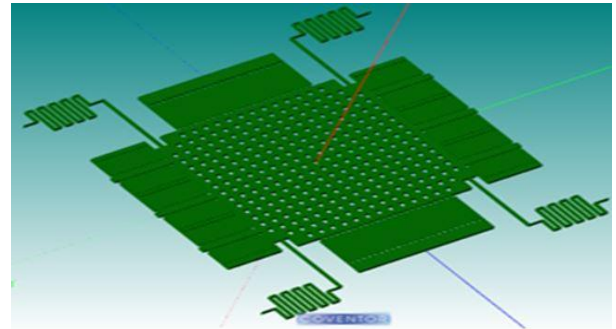


Figure 15. 3 Dimensional Simulated result in MEMS+ window of design 2

A. Modal analysis of Design 2.1

As we can see from the above table that the values of resonant frequencies have come down from 10 KHz to 4 KHz. The modal frequencies are as follows.

TABLE IV. SHOWS THE MODAL FREQUENCIES OF THE DESIGN 2.1 WITH CHANGES INCORPORATED.

Modes	Frequencies in KHz
Sense	4.079
Drive	4.165
Z axis	5.381

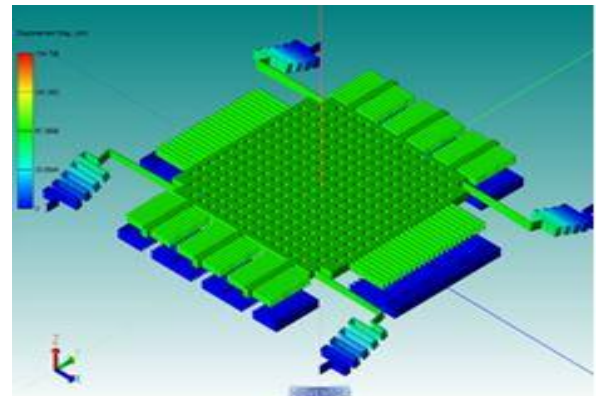


Figure 16. Resonant frequency along Z axis of Design 2.1.

B. Modal analysis of design 2.2 with increased serpentines

With the previous design 1.1 as reference and only changing the length of serpentines maintaining other things as they were previously concluded in the design 1.2. Here we increased the serpentines length to 600 microns along y axis as shown in figure.



Figure 17. Increase in the serpentines along 4 flexures in MEMS+window of design 2.2.

There is a drastic change in the modal frequencies with increase in the number of serpentines with the same dimensions. The resonant frequencies along sense direction has been reduced from 4.079 KHz to 2.358 KHz indicating the increase in sensitivity. And also along the drive axis and Z axis also a noticeable change in the resonant frequency has been observed. The modal frequencies are as follows:

TABLE V. THE MODAL FREQUENCIES OF THE NEW DESIGN WITH CHANGES INCORPORATED IN DESIGN 2.2

Modes	Frequencies in KHz
Sense	2.358
Drive	3.391
Z axis	3.547

The displacement for the design is 0.010075 microns. As can be seen from the simulated results there is no satisfactory displacement as required for our specified design. So still changed the design as follows.

IV. DESIGN 3

The displacement is still not increased so in order to make it more flexible included serpentines again as shown below.

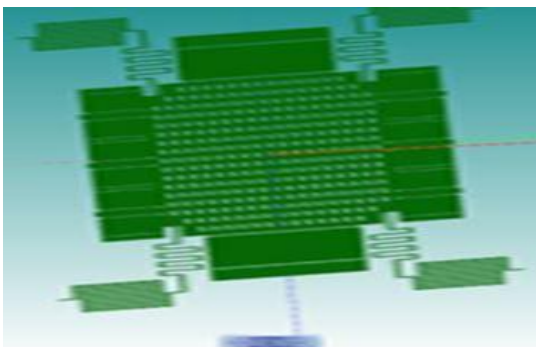


Figure 18. Serpentines included along both beams of the L- Suspension.

The modal frequencies are 2.10 K Hz, 2.803 K Hz and 2.828 K Hz along drive , Z axis and sense respectively.

TABLE VI. MODAL FREQUENCIES OF DESIGN1.3.

Modes	Frequencies in K Hz
Drive	2.10
Z axis	2.803
Sense	2.828

The displacement for the design (1.3) is 0.08 micron for the applied voltage of 5 V. Currently working on the design to match the frequencies and also the displacement towards the design specifications given. Also working on damping effects for the same design where both squeeze and slide film damping are taken into consideration.

ACKNOWLEDGMENT

This research is supported by organization and individuals, I would like to acknowledge the following for technical discussions: FTD Infocom Pvt Ltd and RV College of Engineering; Rakesh Ravindra Naik, Technical Manager and Rajesh P , Senior Application Engineer.

REFERENCES

- [1] JOURNAL OF MICROELECTROMECHANICAL SYSTEMS, VOL. 14, NO. 4, AUGUST 2005 707 A Single-Crystal Silicon Symmetrical and Decoupled MEMS Gyroscope on an Insulating Substrate Said Emre Alper and Tayfun Akin, Member, IEEE
- [2] N. Barbour, G. Schemidt, "Inertial sensor technology trends," IEEE Sensor Journal, vol.1, no.4, pp. 332-339, Dec. 2001., Y. Yazdi, F. Ayazi, and K. Najafi, "Micromachined inertial sensors," in Proceedings of IEEE, vol. 86, no.8, pp.1640-1659, August 1998.
- [3] A LOW-COST RATE-GRADE NICKEL MICROGYROSCOPE S. E. Alper, K. M. Silay, and T. Akin* Middle East Technical University, Dept. of Electrical and Electronics Eng., Ankara, Turkey. Sensors and Actuators A:Physical. 8 November 2006, Pages 171–181, The 19th European Conference on Solid-State Transducers.
- [4] Dynamic Characteristics of Vertically Coupled Structures and the Design of a Decoupled Micro Gyroscope Bumkyoo Choi , SeungYop Lee , Taekhyun Kim and Seog Soon Baek, Lee, B.; Oh, Y.; Park, K.; Ha, B.; Ko, Y.; Kim, J.; Kang, S.; Choi, S.; Song, C. A dynamically tuned vibratory micromechanical gyroscope accelerometer. Proc. SPIE smart electronics and MEMS(Australia, 1997) 1997, 3242, 86–95. [Google Scholar]. Sensors (Basel). 2008 Jun; 8(6): 3706–3718
- [5] Design of MEMS Gyroscope for Wide Range Resonance Frequency Adjustment Manut, A*, Zoofakar, A. S*, Mohd Kharuddin, K.N., Zolkapli, M*, and Abdul Aziz, A* *Faculty of Electrical Engineering Universiti Teknologi MARA Shah Alam, Selangor Darul Ehsan _Institute of Microengineering and Nanoelectronics (IMEN), Universiti Kebangsaan Malaysia, Selangor.Semiconductors Electronics(ICSE),2010 IEEE International conference.
- [6] High aspect-ratio polysilicon micromachining technology Farrokh Ayazi), Khalil Najafi Center For Integrated MicroSystems, Department of Electrical Engineering and Computer Science, University of Michigan,1301 Beal Alenue, Ann Arbor, MI 48109-2122 USA Received 30 December 1999; received in revised form 20 March 2000; accepted 25 March 2000. Sensors and Actuators 87 _2000. 46–51.

- [7] Xie, H. and Fedder, G. (2003). "Integrated Microelectromechanical Gyroscopes." *J. Aerosp. Eng.*, 10.1061/(ASCE)0893-1321(2003)16:2(65), 65-75.
- [8] Design and Simulation of MEMS Based Gyroscope Sujit Kumar, B. Hemalatha Department of Instrumentation and Control Engineering, SRM University, KattankulathurChennai, Tamilnadu-603203, India
- [9] Design and Simulation of MEMS Based Gyroscope Sujit Kumar, B. Hemalatha Department of Instrumentation and Control Engineering, SRM University, KattankulathurChennai, Tamilnadu-603203, India
- [10] *IOSR Journal of Electrical and Electronics Engineering (IOSR-JEEE)* e-ISSN: 2278-1676, p-ISSN: 2320-3331, Volume 5, Issue 6 (May-Jun 2013), PP 23-30.



Sudha R Karbari was born in Karnataka, India, in 1986. She received B.E degree in Electronics and Communication Engineering and MTech in Digital Electronics and Communication with MEMS as specialization honors from Visveswaraya Technological University, Belgaum, Karnataka in 2009 and 2013 respectively. Her research interests include MEMS and RF MEMS.

She has a work experience of 1.4 years for an IT firm and teaching experience of 3 years in different institutions as ASSISTANT PROFESSOR Currently She is working as an Assistant professor in R V College of Engineering, Electronics and Communication Department, Bangalore, Karnataka, India.

Mrs Sudha R Karbari is an active member of IEEE and has two publications in International Conferences for the year 2013 and 2014.